

Retrieval of 30-meter high resolution ET from Landsat inputs with spatial and temporal pattern and dynamics analysis of USGS ARD Actual ET

Authors: Reagan Harris¹, Maosi Chen², Wei Gao^{2,3}

¹ Ecosystem Sciences and Sustainability, Colorado State University, Fort Collins, Colorado 80523 USA, (303)-408-1210, Reagan.Harris@colostate.edu

² ColoradoView, USDA UV-B Monitoring and Research Program, Natural Resource Ecology Laboratory, Colorado State University, Fort Collins, CO 80521 USA

³ Department of Ecosystem Science and Sustainability, Colorado State University, Fort Collins, Colorado, 80523 USA

12/2021

1. Introduction

Evapotranspiration (ET) is comprised of evaporation and transpiration measurements for a total water and energy flux exchange from the land surface to the atmosphere. Over a specific region, it can be used as an indicator of the ecosystem's health, hydrologic cycle, agricultural processes, and water dynamics. Because ET is a process driven by energy exchanges between the surface and the atmosphere the main inputs for ET retrieval algorithms are daily surface and air temperatures, both short and longwave radiation, wind speed and height, and relative humidity. In Colorado, the ET measurements can be used for vegetation health and drought indices as well as irrigation schedules and agriculture planning (Allen *et al.*, 1998). Actual ET is the calculation of ET from the product of the reference and fractional ET (Senay *et al.*, 2013). If ET is happening at a rate faster than water is being replenished to the soils, precipitation rate, then the soils and the vegetation will dry out. Depending on the soil's ability to hold water the actual ET is typically equal to the precipitation of the region unless the area is irrigated like the eastern plain of this projects study region, the state of Colorado. To retrieve the actual ET over the study region the Simplified Surface Energy Balance (SSEB) parametrization from Senay *et al.* (2007) is used for its higher efficiency over alternative formulas like the Bowen ratio energy balance and the eddy correlation which focus on requirements like terrain topography, and the Penman-Monteith combination equations and the Priestly-Taylor approximation which are estimation by meteorological variables (Pauwels & Samson, 2006). The SSEB is a thermal approach for ET estimates utilizing the land surface temperature for greater accuracy of actual ET. The operational SSEB or SSEBop builds off the original SSEB algorithm enhanced by Senay *et al.* (2011a) to account for elevation and latitude changes, a factor necessary for retrieval over the Rocky Mountains. This study aims to retrieve and analyze the temporal trend of 30-meter ET over the Colorado region from the years 2000-2018 derived from USGS Landsat data and analyze the spatial and temporal pattern of the USGS actual ET.

2. Data

Table 1

List and characteristics of datasets used in this study.

No.	Source/Satellite/Sensor	Parameter	Frequency	Resolution	Reference
1	Landsat 8 (TIRS) (VNIR)	Land Surface Temperature (T_s), NDVI	Daily (2014 - 2018)	30 m	Irons, Dwyer, and Barsi (2012)
2	Landsat 7 (ETM+) (TIR)	Land Surface Temperature (T_s), NDVI	Daily (2012 - 2013)	30 m	Goward et al. (2001)
3	Landsat 5 (TM) (TIR)	Land Surface Temperature (T_s), NDVI	Daily (2000 - 2011)	30 m	Barsi et al. (2007)
4	Daymet	Air Temperature (T_a)	Daily (2000 - 2018)	1000 m	Thorton et al. (2020)
5	Gridmet	Incoming Shortwave Radiation (R_s) Reference Evapotranspiration (ET_r) Vapor Pressure Deficit (VPD)	Daily (2000 - 2018)	4638.3 m	Abatzoglou (2013)
6	MODIS	Albedo (α)	16 day climatology (0-12)	500 m	Schaaf et al. (2002)
7	ERA5	Wind Speed (u_2)	Daily (2000 - 2018)	27830 m	Copernicus Climate Change Service (2017)
8	SRTM	Elevation (z)	–	30 m	Farr and Kobrick (2000)
9	Counties	County Boundaries	–	–	US Census Bureau
10	NLCD, 2011	Land cover	Annual (2011)	30 m	Yang et al. (2018)

VNIR: Visible and Near-infrared, TIRS: Thermal Infrared Sensor, ETM+: Enhanced Thematic Mapper Plus, TIR: Thermal Infrared, TM: Thematic Mapper, NDVI: Normalized Difference Vegetation Index, MODIS: Moderate Resolution Imaging Spectroradiometer, ERA5: Fifth Generation Daily Aggregate Dataset, SRTM: Shuttle Radar Topography Mission, and NLCD: National Land Cover Dataset.

The original algorithm for the SSEB from Senay *et al.* (2007) used the MODIS Land Surface Temperature 8-Day Global 1km dataset (Terra MOD11A2.005). Senay *et al.* (2015) used the Landsat 8 thermal band 10 to calculate the land surface temperature. For this study the publicly available United States Geological Survey (USGS) analysis ready data (ARD) which provides daily land surface temperature from Landsat was used. Landsat 8 was used for year 2014 -2018 and while it did cover partial months in 2013 Landsat 7 was used for the entire year of 2013 and 2012 with similar issues from Landsat 5 in 2012. Landsat 7 was to be avoided as much as possible from the data gaps in each image because of the scan line corrector (SLC) failure in 2003. The Daily Surface Weather and Climatological Summaries (Daymet) provided the daily minimum and maximum temperature. Daymet is a parametrization of daily estimated weather from meteorological observations (Thorton *et al.*, 2020). The Gridded Surface Meteorological Dataset (Gridmet) from the University of Idaho, which combines the National Land Data Assimilation System (NLDAS) and the Parameter-elevation Regressions on Independent Slopes Model (PRISM) for their spatial and temporal contributions to land surface modeling, was used for its daily reference ET for alfalfa (ET_r) as a validation for the derived reference ET detailed in the methodology section (Abatzoglou *et al.*, 2013). For this study, albedo was obtained from MODIS Albedo Model (MCD43A3.006) which is derived from MODIS surface reflectance and broad-spectrum bands. The MODIS Albedo daily images are each generated from 16 days of data which are centered on the specified day (Schaaf *et al.*, 2002). For wind measurements the fifth generation daily aggregate dataset (ERA5) from the European Centre for Medium-Range Weather Forecasts (ECMWF) provided data for both the u , east/west, and the v , north/south, wind components. ERA5 provides daily aggregated data globally from observations and model data (Copernicus Climate Change Service, 2017). The USGS also provided 30-meter topographic elevation data from the Shuttle Radar Topography Mission (STRM) (Farr and Kobrick, 2000).

2.1 Ancillary Datasets

The National Land Cover Dataset (NLCD) from the USGS provided Landsat-based 30-meter land cover data for multiple epochs (Yang *et al.*, 2018). We used this dataset to identify the cropland in Colorado and to mask out all other land cover types ensuring only well vegetated pixels were remaining. From United States Census Bureau, the 2018 TIGER US Census Counties was used for the Colorado county boundaries to reduce the spatial processing (US Census Bureau, 2018).

2.2 Validation of ET retrievals

To validate this study's actual ET product, we used the Provisional Actual ET product provided by the USGS Earth Resources Observation and Science (EROS) Center Science Processing Architecture (ESPA). This on-demand product is available through the Earth Explorer webpage or through their ESPA API for bulk ET orders using scene lists acquired from the Earth Explorer website. The ET images are a collection 1 level 1 product and provide six bands with metadata.

3. Methodology

Code: <https://code.earthengine.google.com/bf2fb76ceb035203f378287c2578a181>

The actual ET over the Colorado region is diverse due to the multiple land cover types across the state, the harsh seasons, the temperate desert, mountainous system, and the three Landsat sensors used across the temporal range. In the eastern counties of Colorado, many are agriculture and crop farms with irrigation systems creating actual ET values which are unnatural to the temperate desert climate of grasslands in the region. In the validation process six counties spanning across the state were chosen to reduce processing time of thousands of images although statistics for each county are available. The six counties chosen were Denver, Elbert, Gilpin, Moffat, Phillips, and San Juan. Denver and Gilpin are central Colorado counties, Denver being urbanized with buildings, parking lots, roads, and little natural land cover and Gilpin being just west of Denver and about 70% evergreen forest. Moffat and San Juan are mountainous counties with Moffat in the northwest corner of the state about 75% covered in shrubland and San Juan in the southwest corner and is a good mix of land cover types with forests and barren land (rocks, sand, clay). Phillips and Elbert are in the eastern plains of Colorado, with Phillips in the northeast corner and Elbert in the southeast. Phillips is an agricultural county of crop circles and farming plots while Elbert is grasslands with little human footprint or agriculture.

The retrieval process was broken up into the different Landsat sensors that spanned across the range for this study, 2000 – 2018. The years 2000-2011 were covered by Landsat 5, 2012 and 2013 from Landsat 7, and 2014-2018 from Landsat 8. Because of the scan-line corrector error in Landsat 7 imagery, the minimum number of years were evaluated using the land surface temperature from Landsat 7.

For implementation of the SSEBop algorithm the methodology from Senay *et al.* (2015) was followed and a summary of the methodology is depicted in Senay *et al.* (2015, P. 176, Fig. 2). Further explanation of equations like net short and longwave radiation and temperature difference along with constants used in this study were referenced from Senay *et al.* (2013). The algorithm was implemented using the web-based IDE, Google Earth Engine (GEE), which gives public access to geospatial datasets for visualization and analysis. Google Collaboratory was used for batch exporting retrieved images, ordering validation images and statistical analysis.

3.1 Reference ET

To calculate actual ET, the fractional ET is multiplied by a scaled reference ET. The scaling factor used is, k , which is a unitless coefficient that is used to scale the reference ET to the maximum ET experienced by a dynamically rougher crop (Senay *et al.*, 2013). For this study the recommended scalar coefficient of 1.0 for k was used (Senay *et al.*, 2015). For their reference ET Senay *et al.* (2013) used the Global Data Assimilation System (GDAS) from the National Oceanic and Atmospheric Administration's (NOAA) dataset. For this study the Penman-Monteith reference ET combination equation found in the Food and Agriculture Organization of the United States (FAO) Irrigation and Drainage Paper No. 56 paper was used for this study (FAO, 1998, P.19).

3.2 Temperature Correction Coefficient:

Initially, the temperature correction coefficient value (c) suggested for the Colorado River Basin (Senay *et al.*, 2015) was used as a constant for the whole temporal range of the study, 2000-2018. The temperature correction coefficient is used to relate the maximum air temperature to the observed Landsat land surface temperature.

The c value is a sensitive scaling value and small variations in the coefficient can dramatically change the actual ET output. Landsat's 30-meter and Daymet's 100-meter resolutions allowed for increased resolution calculation on a county level. For this study's c value, the daily maximum air temperature from Daymet was used. The USGS National Land Cover Database (NLCD) was used to mask out all land cover that wasn't cropland. Cropland was used for the c value because these pixels would have the purest NDVI which was then restricted to the 99th percentile to include the best pixels regardless of the NDVI value because of the strong correlation between cumulative NDVI and actual ET (0.96) (Cihlar *et al.*, 1991). Because of the small variation in c values between the months, the calculated 16-day values were aggregated in monthly averages each containing at least one value to represent the month, then were further aggregated to seasonal values by the calendar defined seasons. Similar to the 2013 CRB study (Senay *et al.*, 2015), a seasonal value for winter, spring, summer, and fall following the calendar seasons was calculated from aggregated monthly averages.

3.3 Temperature Difference

The temperature difference (dT) equation remained unchanged, but the recommended constants from Senay *et al.*, (2013) were used in this study. The specific heat of air at constant pressure (C_p) ($1.013 \text{ kJ kg}^{-1} \text{ C}^{-1}$) and the aerodynamic resistance to heat flow from a hypothetical bare and dry surface (r_{ah}). Because r_{ah} was found to be spatially uniform by Qiu *et al.*, (1998) the value was set to 110 s/m from a range of 100 – 120 s/m.

3.4 Fractional ET

Fractional evapotranspiration (ET_f) is used as a scaling factor for the reference ET. Calculated from the land surface temperature, the reference hot pixel and the temperature difference the fractional ET is a unitless decimal between 0 and 1. When calculating the fractional ET for a given day, if the land surface temperature was greater than the calculated hot reference pixel the fractional ET would be negative, and any negative value was set to 0 following the recommendation from Senay *et al.* (2013) as well as any value above 1.05 was masked out.

3.5 Validation Dataset

For the validation dataset, Google Collaboratory was used to stack the separate bands into a single image and import each image into an image collection in the GEE assets for visual validation against our retrieved ET. The bands that were chosen to stack and used in the validation process were the actual ET (ETa), fractional ET (ETf), ET Uncertainty (etun), and Pixel Quality. This validation process was chosen because the USGS EROS estimation for their actual ET is the same SSEBop parametrization used in this study. Notably, for their reference ET they chose the alfalfa ET reference band from Gridmet was used for validation of our derived reference ET from FAO 56.

4. Results and discussion:

4.1 USGS Analysis Ready Validation Data

4.1.1 Long-term dynamics of USGS Analysis Ready Data actual ET in Colorado

To assess the actual ET trend over the range of this project (2000-2018), the annual average values for USGS ARD actual ET from Landsat 5, 7 and, 8 were combined (Appendix E, Figure 1). The annual daily ET mean was 1.68mm per day with the highest annual average in 2014 (2.14mm day⁻¹) and the lowest in 2003 (1.25mm day⁻¹). Landsat 8 years (i.e., 2014-2018) had a higher annual average than Landsat 5 (i.e., 2000-2011), which could mean the later years saw more precipitation or the difference in sensors are creating variation within the actual ET estimation. The years 2000, 2007, and 2009 were random peaks in Landsat 5 with means of 1.82mm, 1.61mm, and 1.88mm per day respectively while the remaining years averaged around 1.47mm per day.

Table 2

Linear regression to quantify the trend of actual ET over the 19-year period.

Statistic	Total Landsat (2000-2018)	Cropland	Grassland	Forest	Shrubland
Slope	0.02	0.03	0.02	0.01	0.02
Intercept	-44.39	-50.46	-44.17	-16.73	-28.69
R Square	0.27	0.13	0.13	0.06	0.17
P-Value	0.02	0.12	0.13	0.31	0.07
Standard Error	0.01	0.02	0.01	0.01	0.01

To analyze whether the rate of actual ET was increasing over the 19 years of this study a linear regression was produced between the years and the 19 annual actual ET aggregated values. This regression was also done for the four land cover types to compare their trends with the total Landsat trend (Table 2). The total Landsat had a slope of 0.02 over the 19 years indicating a slow increase of actual ET from 2000 -2018 as well as grassland and shrubland. Cropland had a slightly larger slope potentially indicating the growth of cropland throughout the state in the past 19 years. The slightly smaller slope of the forest land cover could be attributed to multiple factors like the increase of forest fires, the decrease of snowpack, or the increased gentrification of mountain towns (Pederson *et al*, 2013). However, for each land cover type we cannot reject the null for the reason of the p-values being greater than 0.05 indicating that each trend is neither increasing nor decreasing.

Daily ET values were also aggregated into annual mean daily values for each land cover type over the 19 years of this study to assess the similarities in trends against the overall Landsat annual means (Appendix E, Figure 2). Visually, the cropland trend line resembled the total Landsat trend the best with

similar peaks in 2007, 2009, 2014, and 2016 and lows in 2002, 2006, and 2017, however, the cropland average annual values were consistently larger than the overall Landsat averages by 0.75mm in the lows and 1.5mm in the peaks (Appendix E, Figure 1). The remaining land cover types, grassland, shrubland, and forest, all had similar mean trend line values to the overall Landsat, around 1.5mm. Interestingly, the only significant peak in the grassland land cover was in 2009 at 1.86mm which was not experienced in the forest or shrubland. Similarly, the forest land cover had a peak in 2014 at about 2.00mm which was also seen in the total Landsat trend but not experienced by grassland or shrubland.

Table 3

Kullback-Leibler divergence of each Land Cover type from the total Landsat in monthly aggregates over the 19 years of this study.

Land Cover Type	KL-divergence
Cropland	2.51
Grassland	0.08
Forest	0.23
Shrubland	1.79

To evaluate the mean difference between individual land cover types and the overall Colorado region, the probability distribution functions were created based on their monthly aggregated values in the growing season over the 19-year period. A KL-divergence was calculated to quantify each land cover type's divergence from the general Colorado distribution. A KL-divergence is statistical measure of how one probability is different from a reference probability also known as relative entropy. A value closer to 0 means our land cover type distribution is more closely matched with our overall Colorado distribution. Table 2 lists the calculated KL-divergence values. The results indicated that grassland had the least divergent probability distribution (0.08) to the overall Colorado region which is exhibited by visual comparison between the annual trend (Appendix E, Figure 1) and the similar peaks in 2000, 2009, and 2015 (1.70, 1.91, and 1.96mm day⁻¹ respectively) (Appendix E, Figure 2). Cropland had the most divergent probability distribution (2.51) to the overall Colorado region with a total annual mean of 2.67mm per day for cropland with peaks and lows in similar years but with greater averages of 0.50 to 1.50 mm per day (Appendix E, Figure 1 & Figure 2).

4.1.2 Seasonal spatial dynamics of USGS Analysis Ready Data actual ET in Colorado

The trend for the grassland, shrubland and forest were all similar throughout the Landsat's with peaks in June and lows in the winter months. Forest had larger actual ET average values than grassland and shrubland with highs between 2.00 – 2.50mm per day in June while shrubland and grassland both peaked around 2.00mm per day in June (Appendix E, Figure 3). The total monthly averages across each Landsat had a sinusoidal trend with January and December as lows, 1.05mm and 0.80mm respectively, and June as the peak at 2.07mm per day (Appendix E, Figure 4).

Spatially for the USGS Landsat 5 data, the cropland county, Phillips, had the highest average monthly actual ET with a few monthly means greater than 3.00mm in the peak growing seasons, June – August, with an overall average of 1.71mm per day (Appendix C, Figure 3). The grasslands, Elbert County, had little variation between the months of Landsat 5 with peak monthly averages in March and June, 1.74 and 1.81mm per day respectively, and overall average at 1.03mm. With both Moffat and Gilpin being mountainous counties there were few days in the winter months, January – March, that returned actual

ET values due to natural factors (i.e., clouds, snow, etc.). Shrubland and forest counties had similar temporal trends in actual ET with values increasing until their peak in June, around 2.00mm per day, and then decreasing into winter with lows around 0.20mm per day in December (Appendix C, Figure 3). Expectedly, the USGS actual ET uncertainty for each land cover type is lowest in the summer/growing season and highest in the winter months for Landsat 5 (Appendix C, Figure 4). Landsat 7 had comparable seasonal trends for each land cover type except shrubland which did not peak and remained consistent around 1.24mm per day in the growing season, however, there were available dates before March (Appendix B, Figure 3). Landsat 8 had a higher peak for grassland in May (2.64mm day⁻¹) which was not seen for Landsat 5 or 7 and similar to Landsat 7, shrubland did not have a peak throughout the growing season but remained consistent around 1.75mm per day. For Landsat 8 the peak for cropland (3.72mm day⁻¹) was the largest peak among Landsat 5 and 7 (Appendix A, Figure 3) which could describe the greater annual averages for Landsat 8.

4.2 Retrieval Validation

4.2.1 Landsat 5

For Landsat 5 the correlation between our retrieval and the validation data from the USGS. From a monthly aggregation across each year, one point for each month in each year ($n = 144$), the R^2 value was 0.40 (Appendix C, Figure 1a). In a seasonal aggregation the R^2 value was a more acceptable 0.62 (Appendix C, Figure 1b). The cumulative average values for our retrieval ET are consistently greater than the validation averages, however, the linear relationship, especially from a seasonal perspective, indicates the precision of our retrieval with a small oversight in the methodology (Appendix C, Figure 1c). The variation in the monthly values tightened in the seasonal aggregation with grouping of growing season averages separating from the lower winter values following trends of the USGS actual ET.

A temporal analysis of annual means from Landsat 5 shows the trend of our retrieval against the USGS validation data (Appendix C, Figure 2). The retrieval annual daily means vary from 3.0mm (std = 0.64) in 2005 to 4.1mm (std = 0.81) in 2000 which is significantly higher than the validation daily averages of those year, 1.4mm (std = 0.81) and 1.7mm (std = 1.0) respectively. The overall average actual ET of Landsat 5 is 3.3mm from the retrieval and 1.3 from the validation. While the actual ET lines differ by an average of 2mm over the temporal range of Landsat 5, the trends of each are relatable and further showcase precision of the retrieval method along with its bias. The average standard deviation for the retrieval is 0.71 and 0.80 for the validations data. The error bars in Figure 2, Appendix C are two standard deviations from the mean of each year. The smaller standard deviation from the retrieval dataset suggests a more precise methodology for actual ET.

4.2.2 Landsat 7

Because of SLC error in Landsat 7 imagery, this dataset was used as little as possible. Landsat 5 ended mid-2012 and Landsat 8 began early 2013 leaving Landsat 7 the only dataset with complete imagery for 2011 and 2012. Comparison between the two years continues to exhibit larger retrieval actual ET values, but in a seasonal average assessment the grouping of the two datasets remains tight. Similarly, in the monthly average comparison (Appendix B, Figure 1a) the general grouping of the mean values is persistent while variation within the correlation increases. Though the correlation between the retrieval and validation dataset is not strong ($R^2 = 0.20$), the observation of a consistent bias within the retrieval methodology between Landsat 5 and 7 stands (Appendix B, Figure 2)

4.2.3 Landsat 8

The Landsat 8, correlations between the retrieval and validation dataset had larger error between groups with greater variability between the average actual ET values, but the temporal trend of the retrieval matched well with the validation (Appendix A, Figure 2). For the cumulative average over Landsat 8 the retrieval model underestimated the actual ET, compared to the validation data, by 4% with overall averages of 1.67mm for the retrieval and 1.74mm for the validation. The monthly and seasonal cumulative averages both had high variances (Appendix A, Figure 1a and 1b) with correlations of 0.10 and 0.13 respectively suggesting the retrieval methodology of Landsat 8 had higher accuracy, but weaker precision.

4.3 Error analysis

The constant bias in the retrieval methodology covering Landsat 5 and 7 could be found in either the temperature correlation coefficient (c), the shortwave radiation equations, or the potential/reference ET.

4.3.1 Temperature Correction Coefficient

With the c coefficient value being fixed in the Senay *et al.*, (2013) and (2015) (0.985 and 0.993 respectively) the decision to calculate a seasonal value for each year was made to estimate the temperature correlation more accurately between the reference cold pixel and the daily maximum air temperature. Senay *et al.* (2013) focused on seasonally averaged c values using only pixel with a Normalized Difference Vegetation Index (NDVI) of 0.8 or greater and found that spatially the correction coefficient varied minimally. There is a direct correlation between NDVI and other ecological processes such as ET especially in the growing season with cumulative NDVI and actual ET reporting an r value of 0.96 (Cihlar *et al.*, 1991). Although similar results were found in a spatial determination of c from a previous intern, temporally the mean correction coefficient varied as much as 0.5 in the growing season with standard deviations reaching from 0.93 to above 1.0 (Appendix D, Figure 1). However, the previous student intern had a bias in their retrieval. For the daily maximum air temperature, they used the same Daymet dataset, but they had fixed a constant day for the maximum air temperature, a day at the end of the growing season in August. This decision was undocumented and impractical for its application. In our coefficient retrieval the same equation from Senay *et al.* (2013) was used and the maximum air temperature was adjusted to the daily maximum air temperature for the given day. Our retrieval, using the 99th percentile of NDVI pixels, returned little variation temporally and spatially with all seasonal averages around 0.99 (Appendix D, Figure 2). Our seasonal average is, however, too large and is speculated to be the source of the bias in the Landsat 5 retrieval. Lower c values will produce smaller actual ET estimates and is needed to bring our retrieval averages closer to the validation measurements. When a constant c value of 0.97 was tested in our retrieval the annual average actual ET was much closer to the validation, but still overall larger than the validation measurements. Using a constant c value like 0.985, suggested in Senay *et al.* (2015) for the CRB study, would reduce the retrieved actual ET values but not enough to make being within 10-20% of the validation data.

A notable difference between the c value retrievals is the slope and trend of the monthly aggregated c values. The previous intern's c value created a sinusoidal arch with minimum means in January and December and a peak in July (Appendix D, Figure 1). Our c value retrieval better resembled the c value plot in Senay *et al.* 2013 (Figure 2), which does not have an obvious seasonal shape rather a random

noise surrounding the mean value. The differences between the method of retrieval for the c value is Senay *et al.* (2013) used data from about 6-7 years (number of samples = 2,174 days) and excluded the winter months September through March, while our retrieval used values from 12 years and did not exclude any months. For calculating a daily c value, a suggestion for future work is to use the coldest pixel in the region for that day for the land surface temperature and the warmest pixel for the same parameters for the maximum air temperature. Doing so created an average 0.965 and will produce significantly lower actual ET values. The coefficient value and its parameterization need more research into the c value formulas, how they are affected by each variable, and which dataset are used. The high c values, around 0.99, are attributed to the high retrieval values for Landsat 5 and we speculate this to be the source of bias in this study.

4.3.2 Reference Hot Pixel

The hot reference pixel is the sum of the cold reference pixel and the temperature difference. The hot reference pixel calculation is the source of two possible biases; the correction coefficient, controlling the cold reference pixel, and the temperature difference which is primarily derived from the clear-sky net radiation. Net shortwave radiation is used to calculate temperature difference (dT) and the hot reference pixel. If the hot reference pixel is greater than the land surface temperature the fractional ET will be negative and set to 0 by recommendation from Senay *et al.* (2013). With most pixels set to 0 the actual ET estimation will be underestimated. Net shortwave radiation was initially calculated using Daymet's incident shortwave radiation flux density band, however, rough transitions in the band across the Colorado region produced an overabundance of negative fractional ET values. Having eliminated the possibility of cloud cover/shadow by applying the Landsat bitmask to the Daymet dataset and noting that this pattern persisted throughout the temporal range of the dataset, a new method to obtain net shortwave radiation was needed. The second attempt was with Gridmet's incoming shortwave radiation band was made. This attempt returned fractional ET values far above the suggestion maximum of 1.05 by Senay *et al.* (2013). The possibility of the error stemming from the longwave radiation was dismissed as net longwave radiation had little variation throughout the study and the equations were followed from Senay *et al.* (2013). Finally, the net shortwave radiation was calculated following the equations in Senay *et al.* (2013) which did create a range of fractional ET values close to the validation dataset. While this method did seemingly solve the shortwave radiation issue and thus the fractional ET, a validation dataset for net shortwave radiation should be found and used to ensure there is not bias from this methodology.

4.3.3 Penman-Monteith Reference ET

The Penman-Monteith reference ET (ETo) equation was not directly used in the Senay *et al.* (2015) paper rather the National Oceanic and Atmospheric Administration (NOAA) Global Data Assimilation System (GDAS) was used for its 100 km ETo . The dataset accessible through GEE was GLDAS or Global Land Data Assimilation System which did have the potential ET rate band. However, the daily aggregated ETo values had averages around 10mm, far above the average from the USGS ET data (5-7mm) which used the Gridmet *alfalfa* reference ETo band. The Penman-Monteith equation found in FAO No. 56 (FAO 56, 1998, Pg. 19) was used for a more accurate ETo . In the Penman-Monteith equation, variables included net radiation, soil heat flux density, mean daily temperature, wind speed at 2-meters above the surface, actual and saturation vapor pressure, vapor pressure deficit, slope vapor pressure curve (Δ), and the psychrometric constant. All of which would come together for a millimeter per day value. This

method did return reference ET values close to the Gridmet alfalfa ETo band, used in the USGS validation data. Although a trial of actual ET retrieval should be attempted using the same Gridmet band.

4.3.4 Actual/Saturated Vapor Pressure

The maximum and minimum relative humidity was used to calculate the actual and saturated vapor pressure which were used for the saturation vapor pressure deficit (VPD) a variable in the ETo equation. The Gridmet dataset provided the max and min daily relative humidity values and contained bands like saturated vapor pressure deficit for validation of our calculated VPD. In addition to the Gridmet dataset, the 2-meter wind speed and 2-meter daily temperatures from the ERA5 were needed to implement the ETo equation. There was a difference between the actual and saturated vapor pressure equations from the two reference articles, Senay *et al.* (2013) and the FAO 56 paper. The FAO 56 actual and saturated vapor pressure equations both had a constant at the start of the equation, 0.6108 multiplied to the rest of the equation, which was not seen in the Senay *et al.* (2013) equations. There was no supporting evidence that the 0.6108 constant was necessary or not, so we suggest further investigation into this equation. Perhaps the vapor pressure equations are based on elevation or similar factors. In addition to the ETo algorithm, the actual vapor pressure equation from relative humidity was also used in the SSEBop parametrization for the longwave radiation equation for consistency between algorithms.

Conclusion:

The analysis of the USGS 30-meter Landsat Evapotranspiration (ET) Analysis Ready Data showed that the overall trend of actual ET was on a slight increase between 2000 and 2018 though the same conclusion could not be made for each land cover type. The grassland land cover type had the least divergence from the total Landsat trend implying that grassland had the most similar trend and averages to the total Landsat data followed by forest and shrubland with the cropland land cover having the largest divergence from the total Landsat trend. The seasonal aggregation of the total Landsat actual ET daily values generated a sinusoidal curve with an increase from January to a peak in June to a subsequent decline to December. The spatial differences in the monthly aggregated actual ET over the land cover types from the USGS data is as expected with the cropland values the highest in the growing season up to the harvesting season and grassland values having little variation throughout the year with monthly values rising in the summer months and decreasing in the winter alike the forest and shrubland land covers while grassland had less variation between the months leading to a lesser climactic peak.

We also retrieved 30-meter actual ET images over the Colorado region from 2000 – 2018. The operational Simplified Surface Energy Balance (SSEBop) was implemented using Landsat 5, 7 and 8 along with available datasets from Google Earth Engine (GEE) and other ancillary datasets. The retrieval of the actual ET was successful, but due to the large biases and error in the retrieval method, analyzing the temporal and spatial patterns of the retrieved actual ET compared to the USGS available actual ET product, the validation dataset, was inconclusive and continued research on the known issues with the retrieval methodology is needed. While the temporal trend between our retrieval and the validation data was similar, with peaks and dips in the same years, the averages were far off in Landsat 5 and 7. The Landsat 8 retrieval was the nearest to the validation dataset when aggregated to annual averages, with an annual mean difference of 0.0 – 0.5mm from the USGS validation data. While Landsat 5 had an

average annual mean difference of 1.5 – 2.3mm from the USGS validation data. Other aggregations like monthly and seasonal comparisons between our retrieval and the validation data were made further showing the grouping of actual ET values between the growing seasons and the off seasons. Future research should focus on the biases in the methodology here to produce a more accurate retrieval.

Appendix Begins Here:

Appendix A: Landsat 8

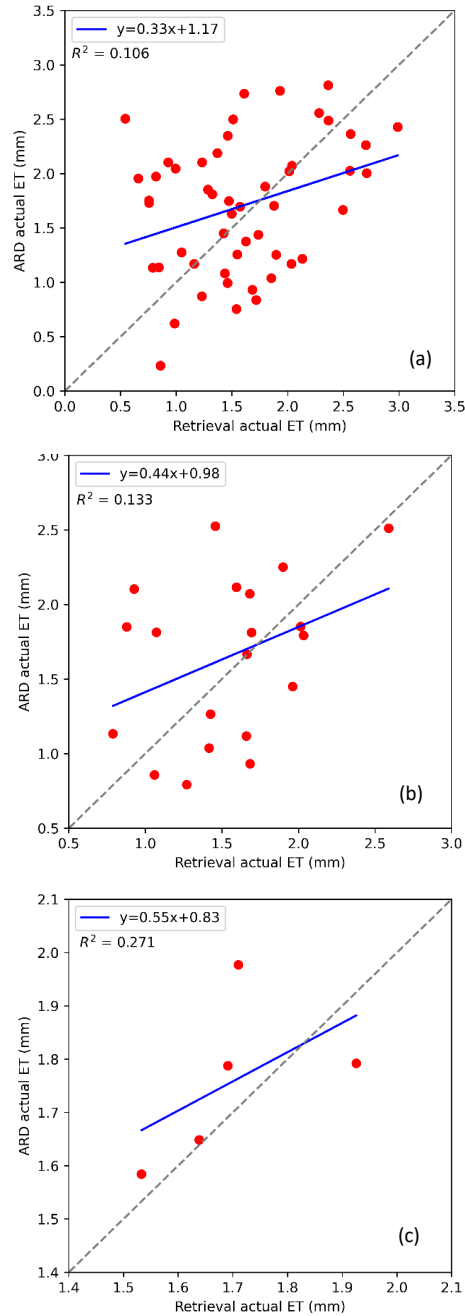


Figure 1. Scatter plot of monthly (a), seasonal (b), and annual (c) retrieved and USGS actual ET for Landsat 8 (2014-2018) with linear regression line (blue) and respective correlation values. The dotted gray line represents a perfect correlation.

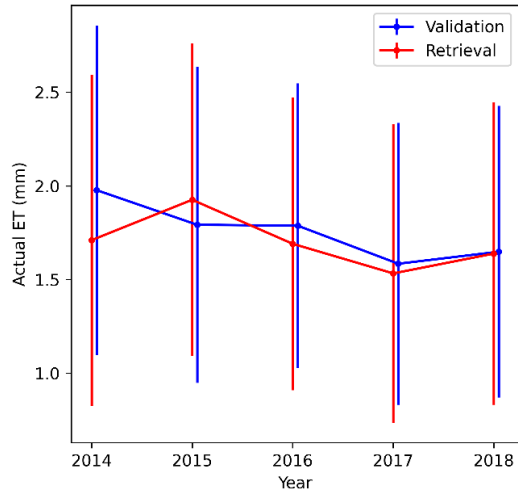


Figure 2. Temporal annual averages of retrieved and USGS daily actual ET from Landsat 8 (2014 – 2018) with annual average daily spatial standard deviation (Error bars).

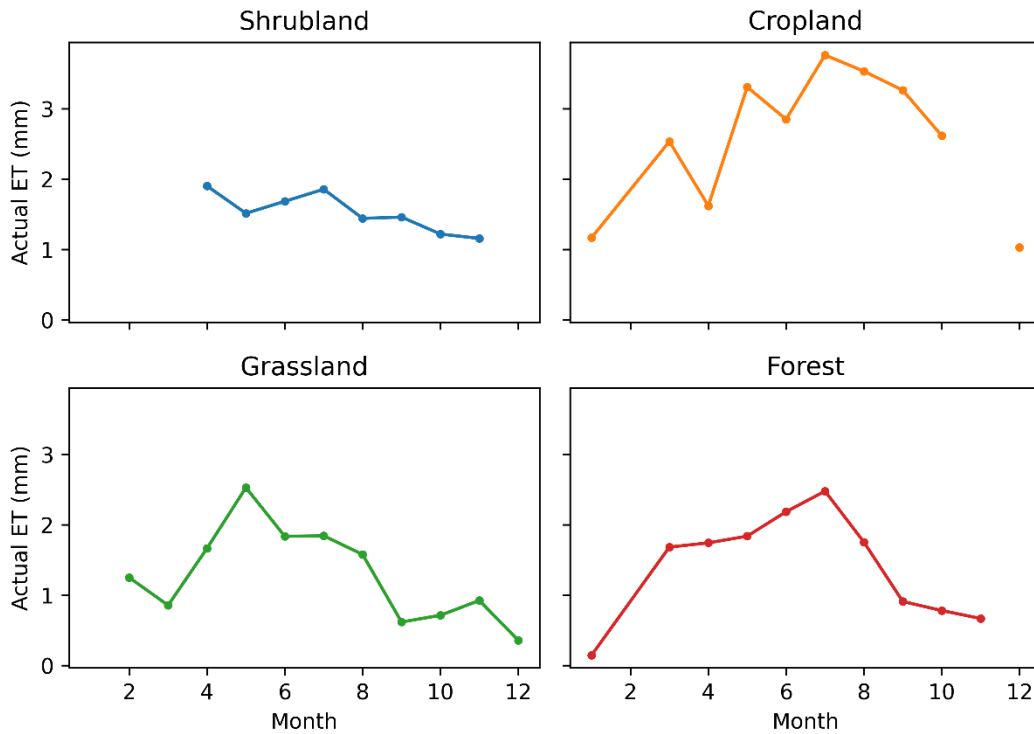


Figure 3. Illustration of monthly averages from USGS actual ET over diverse ecosystems including shrubland, cropland, grassland, and forest for Landsat 8 (2014 – 2018).

Appendix B: Landsat 7

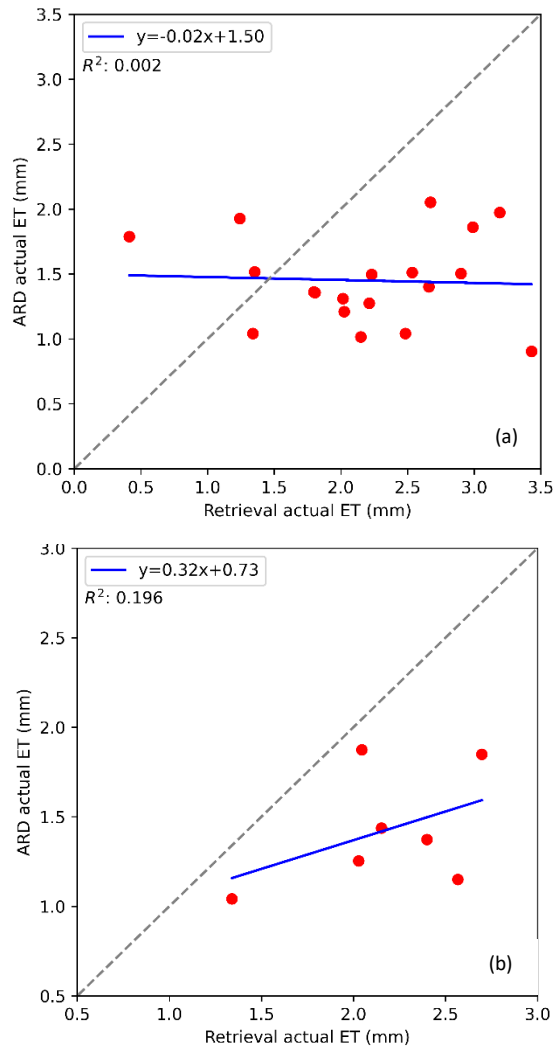


Figure 1. Scatter of monthly (a) and seasonal (b) retrieved and USGS actual ET from Landsat 7 (2012 - 2013) with linear regression line (blue) and respective correlation values. The dotted gray line represents a perfect correlation.

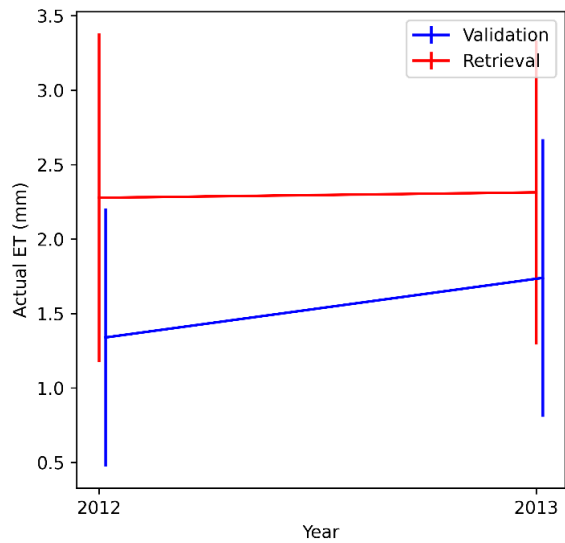


Figure 2. Temporal annual averages of retrieved and USGS daily actual ET from Landsat 7 (2012 – 2013) with annual average daily spatial standard deviation (Error bars).

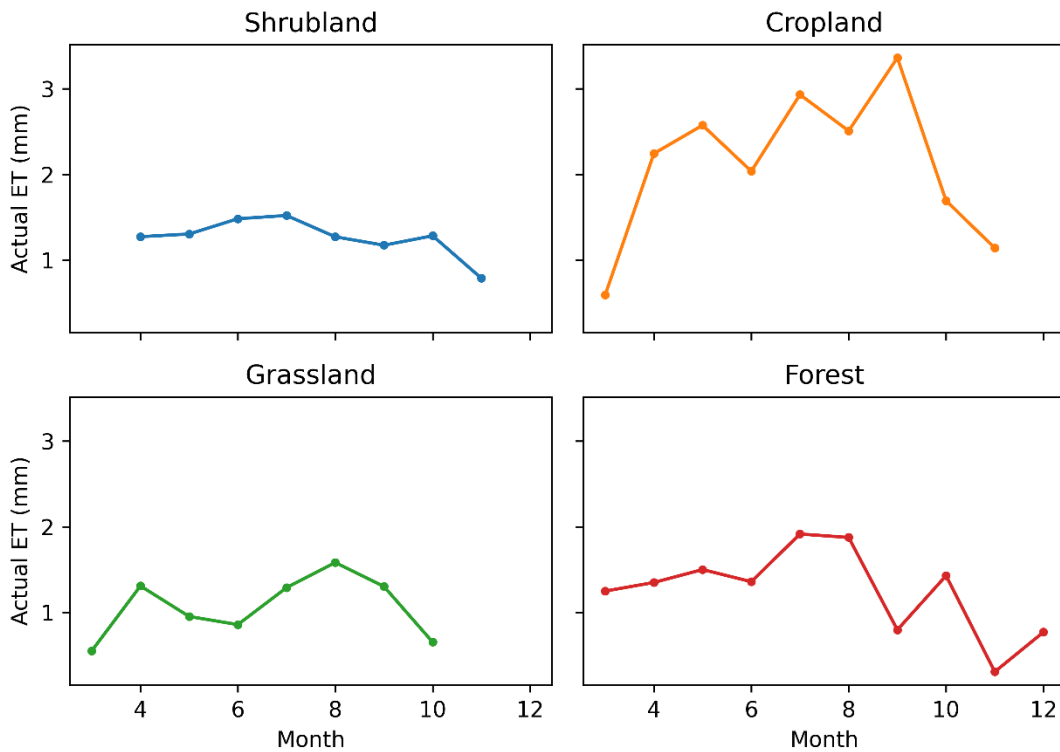


Figure 3. Illustration of monthly averages from USGS actual ET over diverse ecosystems including shrubland, cropland, grassland, and forest for Landsat 7 (2012 – 2013).

Appendix C: Landsat 5

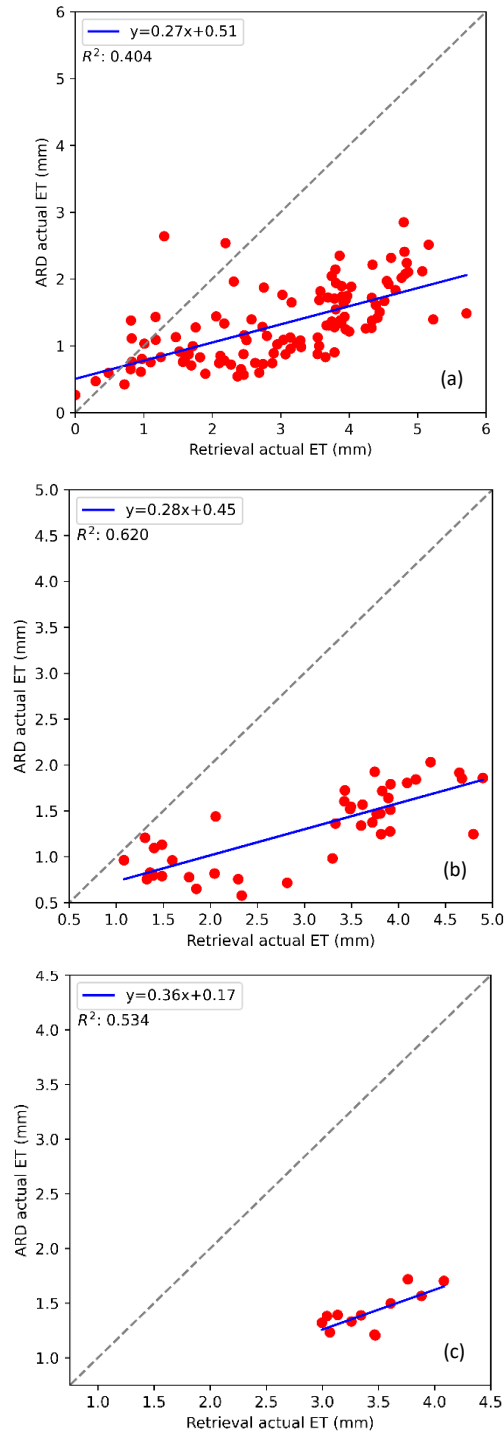


Figure 1. Scatter of monthly (a), seasonal (b), and annual (c) retrieved and USGS actual ET for Landsat 5 (2000 – 2011) with linear regression line (blue) and respective correlation values. The dotted gray line represents a perfect correlation.

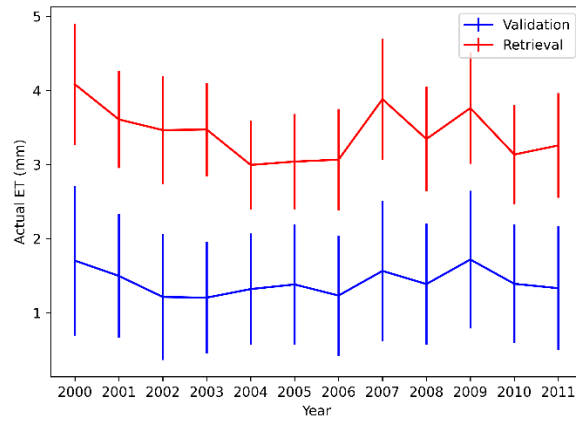


Figure 2. Temporal annual averages of retrieved and USGS daily actual ET from Landsat 5 (2000 – 2011) with annual average daily spatial standard deviation (Error bars).

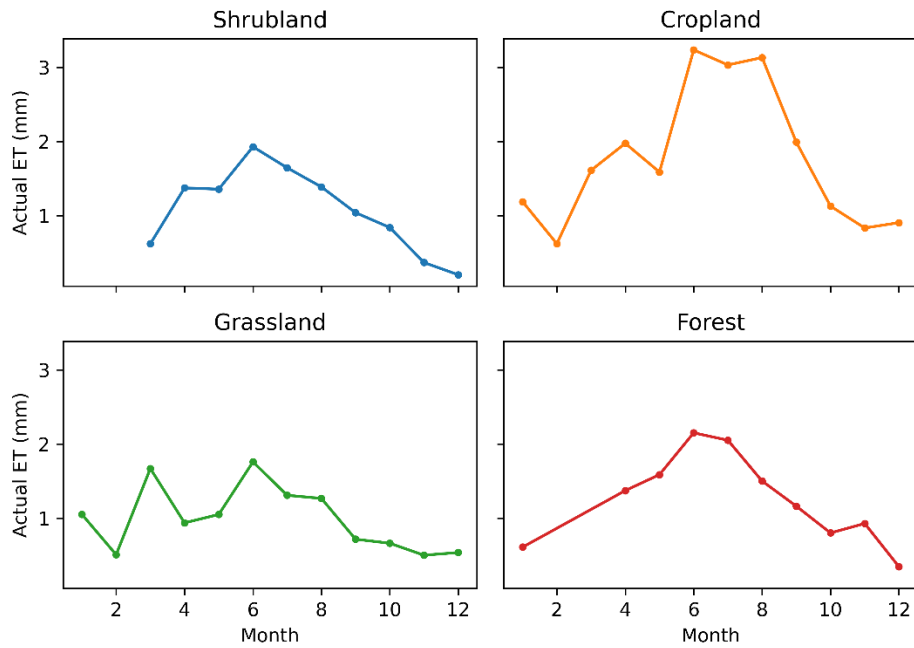


Figure 3. Illustration of monthly averages from USGS actual ET over diverse ecosystems including shrubland, cropland, grassland, and forest for Landsat 5 (2000 – 2011).

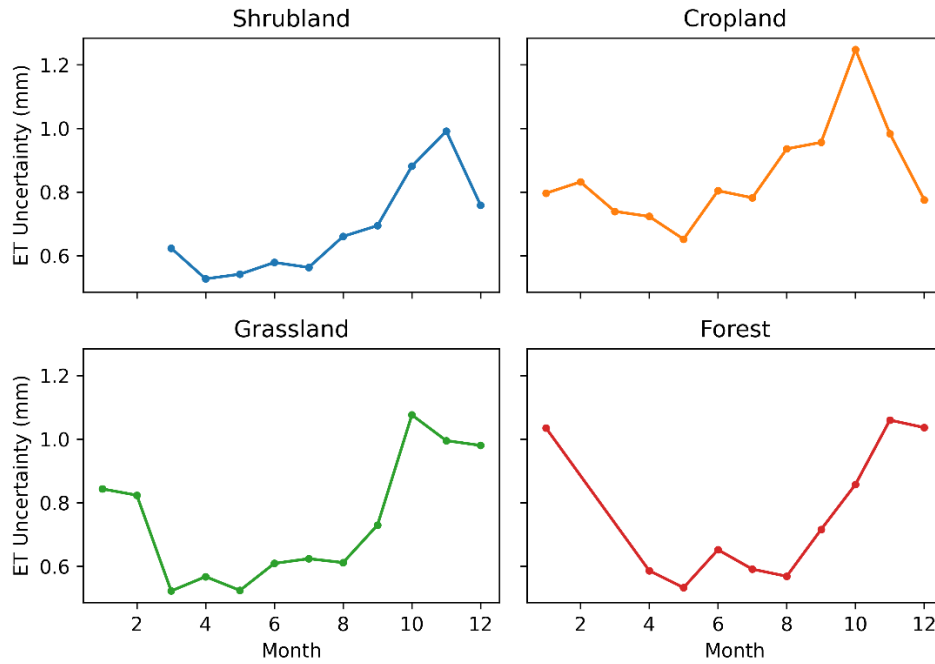


Figure 4. Illustration of monthly averages from USGS actual ET uncertainty over diverse ecosystems including shrubland, cropland, grassland, and forest for Landsat 5 (2000 – 2011).

Appendix D: Temperature Correction Coefficient

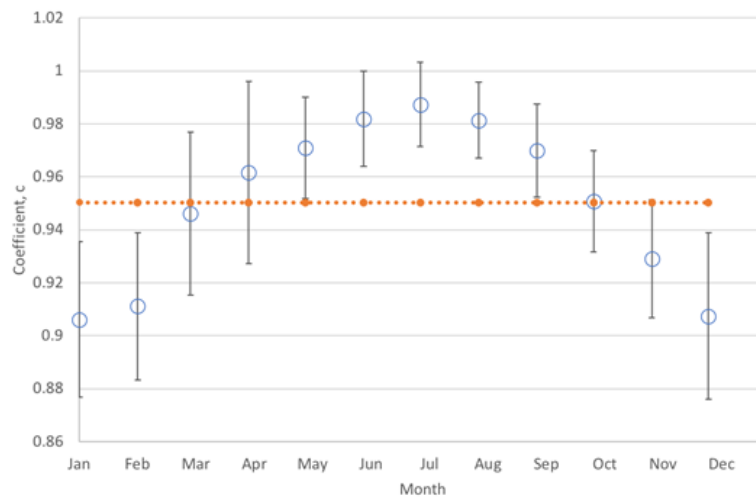


Figure 1. Previous interns aggregated temperature correction coefficient monthly averages with fixed maximum temperature from 2000 -2018 over the whole of Colorado with error bars. The orange dashed line is the average c value.

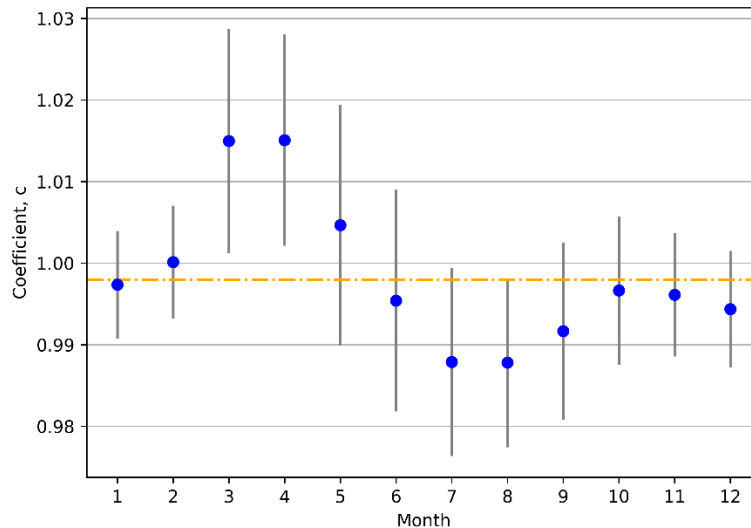


Figure 2. Retrieved temperature correction coefficient (with daily maximum temperature) monthly averages from 2000 – 2018 with standard deviation error bars. The orange line is the average c value of 0.998.

Appendix E: USGS Validation Data

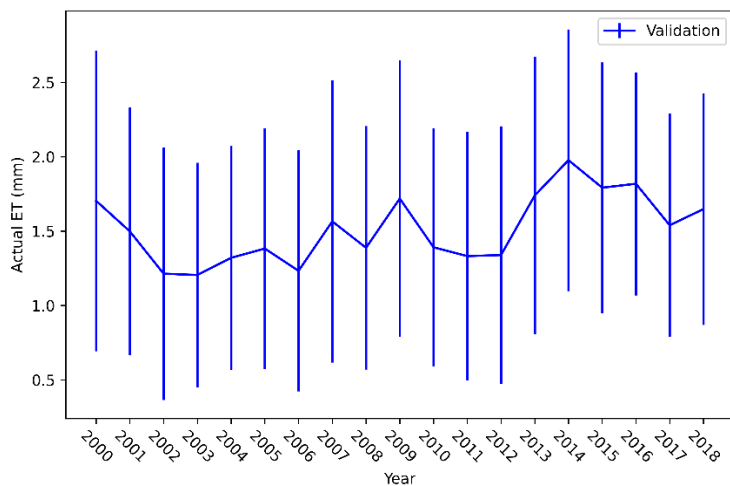


Figure 1. Average annual daily actual ET trend from the USGS actual ET data (2000 – 2018) with error bars of the average daily actual ET standard deviations from the annual mean.

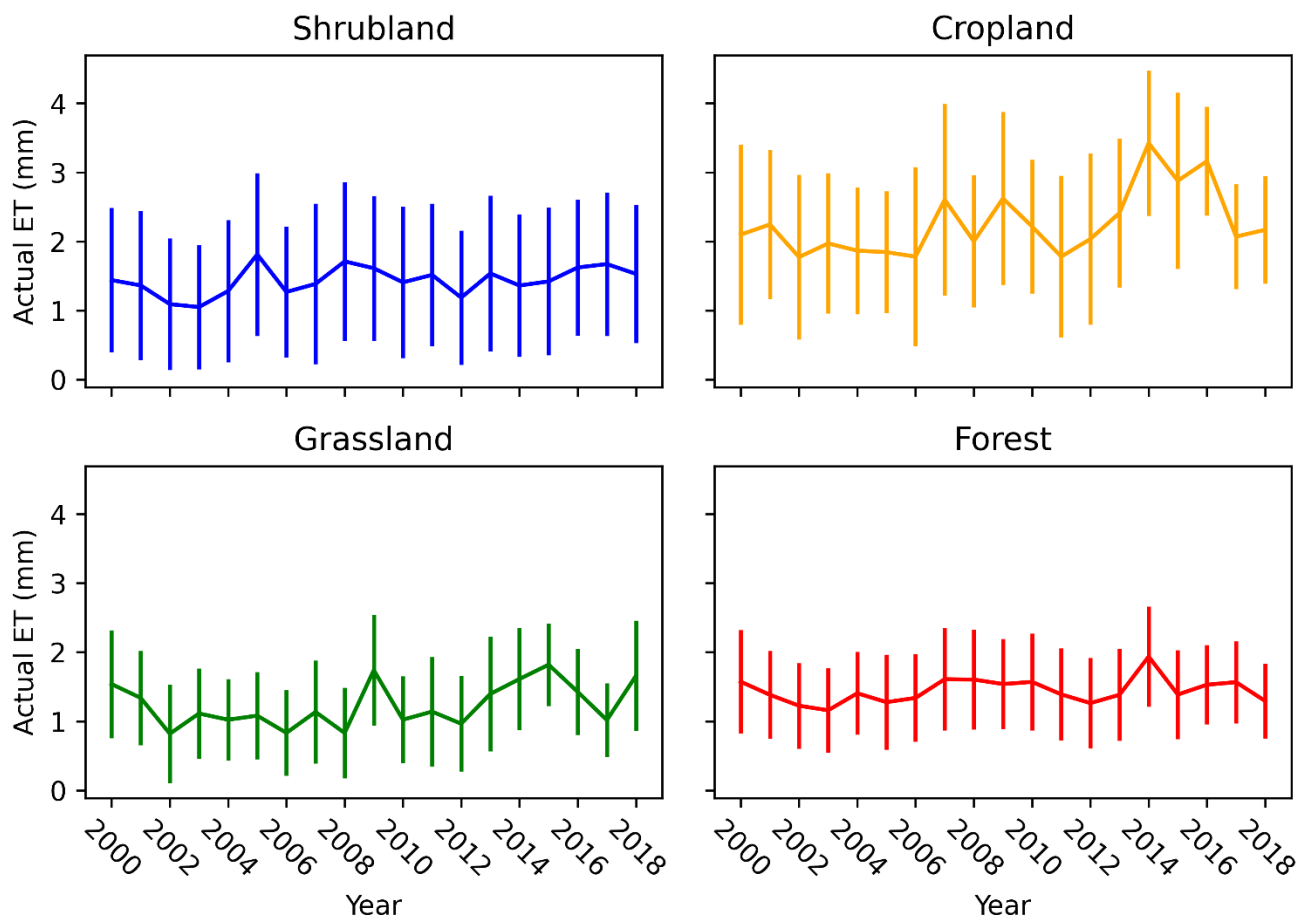


Figure 2. Annual averages of daily actual ET from the USGS validation dataset over the key ecosystems in Colorado across each Landsat (5, 7, and 8). Error bars represent two standard deviations from the corresponding annual mean.

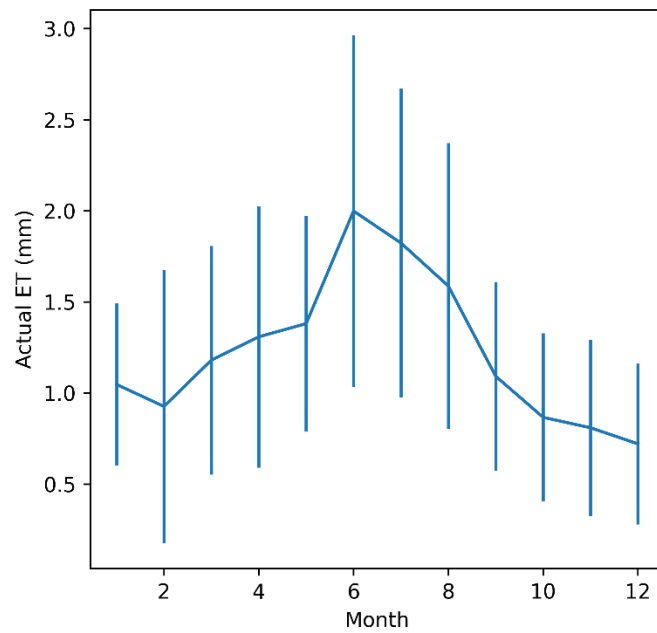


Figure 3. Actual ET daily averages aggregated into monthly means across Landsat 5, 7, and 8. Error bars represent two standard deviations from the mean.

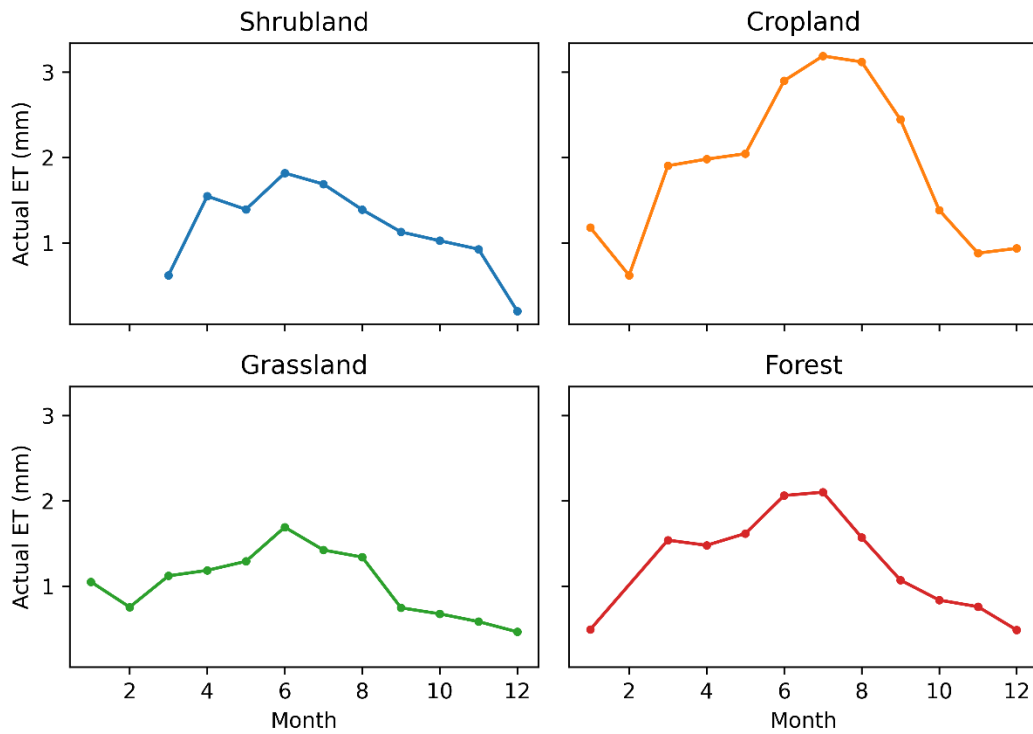


Figure 4. Illustration of monthly averages from USGS actual ET over diverse ecosystems including shrubland, cropland, grassland, and forest for Landsat 5, 7, and 8 (2000 – 2018).

References

- Abatzoglou, J. T. (2013), Development of gridded surface meteorological data for ecological applications and modelling. *Int. J. Climatol.*, 33: 121-131. Doi: 10.1002/joc.3413
- Allen, R. G., Pereira, L. S., Raes, D., *et al.* (1998). Crop Evapotranspiration -Guidelines for computing crop water requirements-FAO Irrigation and drainage paper 56. Fao, Rome, 300(9), D05109.
- Carlson, T. N., Capehart, W. J., & Gillies, R. R. (1995). A new look at the simplified method for remote sensing of daily ET. *Remote sensing of Environment*, 54(2), 161-167. Doi: 10.1016/0034-4257(95)00139-R
- Cihlar, J., Laurent, L. S., & Dyer, J. A. (1991). Relation between the normalized difference vegetation index and ecological variables. *Remote sensing of Environment*, 35(2-3), 279-298. Doi: 10.1016/0034-4257(91)90018-2
- Goward, S. N., Masek, J. G., Williams, D. L., *et al.* (2001). The Landsat 7 mission: Terrestrial research and applications for the 21st century. *Remote Sensing of Environment*, 78(1-2), 3-12. Doi: 10.1016/S0034-4257(01)00262-0
- Irons, J. R., Dwyer, J. L., & Barsi, J. A. (2012). The next Landsat satellite: The Landsat data continuity mission. *Remote Sensing of Environment*, 122, 11-21. Doi: 10.1016/j.rse.2011.08.026
- Jin, S., Yang, L., Danielson, P., *et al.* (2013). A comprehensive change detection method for updating the National Land Cover Database to circa 2011. *Remote Sensing of Environment*, 132, 159-175. Doi: 10.1016/j.rse.2013.01.012
- Pederson, G. T., Betancourt, J. L., & McCabe, G. J. (2013). Regional patterns and proximal causes of the recent snowpack decline in the Rocky Mountains, US. *Geophysical Research Letters*, 40(9), 1811-1816. Doi: 10.1002/grl.50424
- Schaaf, C. B., Gao, F., Strahler, A. H., *et al.* (2002). First operational BRDF, albedo nadir reflectance products from MODIS. *Remote sensing of Environment*, 83(1-2), 135-148. Doi: 10.1016/S0034-4257(02)00091-3
- Senay, G. B. (2018). Satellite psychrometric formulation of the Operational Simplified Surface Energy Balance (SSEBop) model for quantifying and mapping evapotranspiration. *Applied Engineering in Agriculture*, 34(3), 555-566. doi: 10.13031/aea.12614
- Senay, G. B., Budde, M. E., & Verdin, J. P. (2011). Enhancing the Simplified Surface Energy Balance (SSEB) approach for estimating landscape evapotranspiration: Validation with the METRIC model. *Agricultural Water Management*. 98(4), 606-618. Doi: 10.1016/j.agwat.2010.10.014
- Senay, G. B., Budde, M., Verdin, J. P., *et al.* (2007). A coupled remote sensing and simplified surface energy balance approach to estimate actual evapotranspiration from irrigated fields. *Sensors*. 7(6), 979-1000. Doi: 10.3390/s7060979
- Senay, G., Bohms, S., Singh R., *et al.* (2013). Operational Evapotranspiration Mapping Using Remote Sensing and Weather Datasets: A New Parameterization for the SSEB Approach. *Journal of the American Water Resources Association*. 49(3): 577-591. Doi: 10.1111/jawr.12057
- Senay, G., Friedrichs, M., Singh, R., *et al.* (2016). Evaluating Landsat 8 evapotranspiration for water use mapping in the Colorado River Basin. *Remote Sensing of Environment*. 185: 171-185. Doi: 10.1016/j.rse.2015.12.043

- Thornton, P. E., Thornton, M. M., Mayer, B. W., *et al.* (2014). Daymet: Daily surface weather data on a 1-km grid for North America, Version 2. Data set. Oak Ridge, Tennessee, USA: Oak Ridge National Laboratory Distributed Active Archive Center. Doi: 10.3334/ORNLDAAC/1840
- Qiu, G. Y., Yano, T., & Momii, K. (1998). An improved methodology to measure evaporation from bare soil based on comparison of surface temperature with a dry soil surface. *Journal of Hydrology*, 210(1-4), 93-105. Doi: 10.1016/S0022-1694(98)00174-7